## 8

#### **Research Article**

Kareem Dhahir Rahi\*, Leana Jabble Taklef and Musa H. Wali

# Enhancement isolation antenna to multi-port for wireless communication

https://doi.org/10.1515/eng-2022-0348 received April 09, 2022; accepted June 21, 2022

**Abstract:** Currently, there is a rapid increase in demand for the transmission of large amount of data with extreme accuracy, which is usually performed by the antenna system. Therefore, this work aims to design an antenna system that has the potential of improving the performance of such system in terms of reducing the antenna size, and expanding the bandwidth. First, a single-port antenna was designed after calculating the basic requirements and then a comprehensive analysis of the antenna performance was carried out to reach optimum performance. Then, the antenna was connected to two, three, and four ports. Such connection was implemented while maintaining efficiency and magnification in each case within the range for wireless applications. The antenna with four input ports was designed with a 45° angle on a circular circumference around the antenna to prevent interference between the ports. The modified antenna was designed to accommodate wireless communication applications (such as the 5G mobile communications network as well as the future 6G mobile communications network). The experimental results were compared with those obtained from the simulation studio Computer Simulation Technology, which is more compatible with the practical results.

**Keywords:** microstrip antenna, multiple ports, radiation efficiency, power losses

Leana Jabble Taklef, Musa H. Wali: Electronics and Communication Engineering Department, College of Engineering, University of Al-Qadisiyah, Al Diwaniyah, Iraq

## 1 Introduction

The growing demand of data transmission and processing is a constant challenge for the wireless communications community. Such challenge requires continuous development of the existing telecommunications systems. Furthermore, serious and rigorous solutions must be developed to meet the future standards for wireless communications systems, especially 5G. The difference between the modern wireless system and the traditional system is shown by its simple look regardless of the number of processing ports.

There are a number of important requirements that play an important role in the performance of radio systems. One of the most important requirements perhaps is the radiation efficiency of antennas. Although all variables that are related to radiation efficiency of single-port antennas are well documented in previous research, for multi-port antennas, such variables are still debatable to date.

Therefore, this work aims to allocate sufficient time to analyze and discuss the conditions specified in this specialty, which is considered as part of the subject later. The definitions of single-port antennas have been reviewed and expanded to include multiport antennas. It is worth noting the radiation efficiency used in multiport antennas and basic reasons we present. These definitions were made based on the assumption that one active port in a multipoint system can be used from matrix algebra to illustrate some formulas for calculating the useful radiation efficiency [1–11].

# 2 Antenna efficiency description

Generally, an internal resistor can describe voltage sources through its internal contacts. The amount of maximum available power  $P_{\rm avs}$  from the source is fitted to the corresponding load associated with a specific internal resistance source. In multiport antennas, the total  $P_{\rm avs}$  in the opposite ports is the amount of maximum available power. The maximum amount of power provided by the antenna, which is symbolized as  $P_{\rm acc}$ , is called part of the capacity in

<sup>\*</sup> Corresponding author: Kareem Dhahir Rahi, Electronics and Communication Engineering Department, College of Engineering, University of Al-Qadisiyah, Al Diwaniyah, Iraq, e-mail: kareem.rahi@qu.edu.iq

its outlet (or ports) or the amount of available radiation. The state of a single antenna is the difference between the amount of the power accepted  $P_{\rm inc}$  and the reflected force  $P_{\rm rfl}$  for a single antenna.

$$P_{\rm acc} = P_{\rm inc} - P_{\rm rfl}. \tag{1}$$

The amount of power is coupled with the relevant excitement,  $P_{col}^{i}$  for multiport.

$$P_{\text{cp1}}^{i} = P_{\text{inc}}^{i} \sum_{j=1, j \neq i}^{n} |S_{ij}|^{2},$$
 (2)

where  $S_{ij}$  is a fixed entree antenna's scattering matrix, and it is defined as  $S_a(m \times m)$ . Superscript symbol i indicates the port number. The contrary force is known as the amount of reflected force in port i within the incidence area of this port.

$$P_{\rm rfl}^i = |S_{ii}|^2 P_{\rm inc}^i. {3}$$

When port i is excited, the accepted power,  $P_{\rm acc}^i$  suits multiport condition.

$$P_{\rm acc}^{i} = P_{\rm inc}^{i} \left( 1 - \sum_{j=1}^{n} |S_{ij}|^{2} \right). \tag{4}$$

The accepted power in equation (4) represents nocoupling condition, i.e.,  $S_{ij} = 0$  for all j except for j = i, which decreases to equation (1).

 $P_{\rm los}$  represents the partially dissipated acceptable power. The power loss not only depends on the lost portion of the power that reaches the radiation structure, but also depends on the terminal impedance of the other ports in pairing condition. Thus, ohmic losses are not easily determined, since they depend on many specific effects. The rest of the power accepted represents the radiated power ( $P_{\rm rad}$ ) for the ith port [12–15].

$$P_{\rm rad}^i = P_{\rm acc}^i - P_{\rm los}^i, \tag{5}$$

where  $P_{\rm los}^i$  is the power loss when port i is agitated and all other ports are correctly terminated. Note that  $P_{\rm los}^i$  does not include the power dissipated in the terminus of other coupled radiated ports. Likewise,  $P_{\rm rad}^i$  is the radiated power when port i is excited while other ports are terminated. The amount of radiated power is shown in Figure 1 and the amount of power accepted is shown in Figure 2. Figure 3 shows the power loss at the far-field region of the antenna.

## 3 Antenna efficiency depiction

Radiation efficiency is one of the main performance measurements of the antenna, which shows the effectiveness of the antenna in converting the electrical energy in the port to electromagnetic radiation. In other words, the efficiency of an antenna is the ratio of the radiated energy  $P_{\rm rad}$  to the accepted power  $P_{\rm acc}$  by the antenna. The state of the radiation structure without loss represents the efficiency of radiation.

## 3.1 Single-port antenna

Figure 4(a) shows the simulated single-port antenna, while Figure 4(b) displays the fabricated antenna. The total maximum radiation efficiency is 97% in a single-port antenna as shown in Figure 5. Not that, there are no information regarding losses, the figure only shows antenna compatibility with the internal resistance of the feeding source.

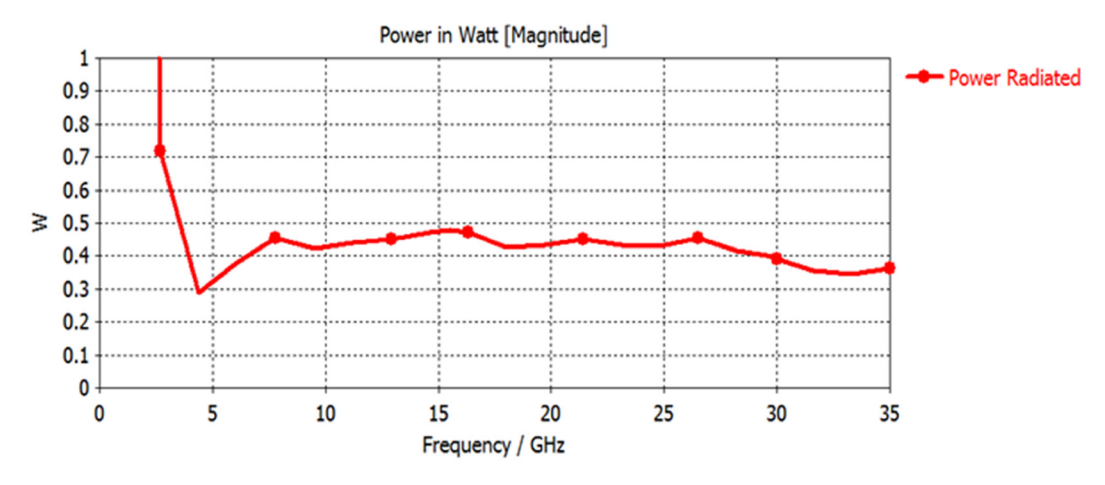


Figure 1: Radiated power for a single-port antenna.



Figure 2: Accepted power for a single-port antenna.

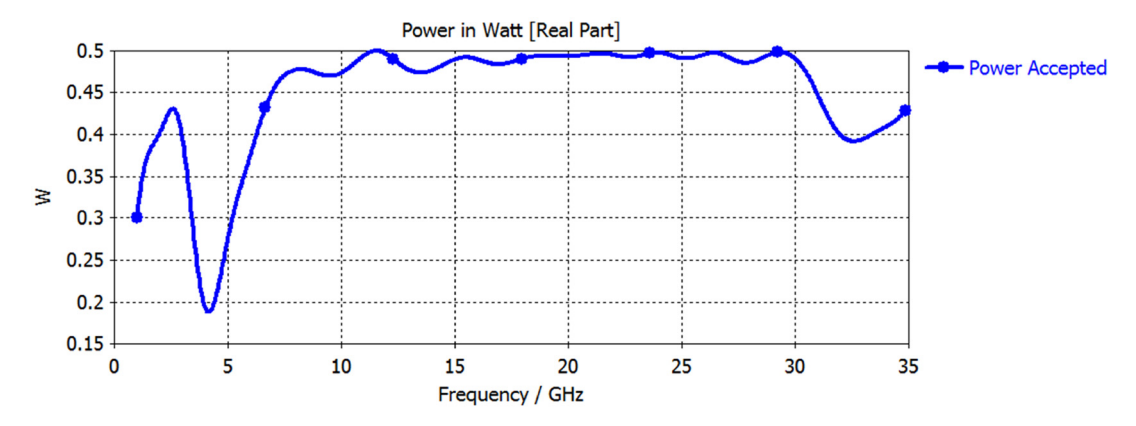


Figure 3: Power losses for a single-port antenna.

The ratio of total radiation efficiency to radiation efficiency is an indication of impedance match ( $e_{\rm mch}$ ), which can be expressed as:

$$e_{\text{tot}} = e_{\text{mch}} \cdot e_{\text{rad}}$$
 (6)

## 3.2 Multiport matching efficiency

The matching efficiency of multiport is a multiple copy of the traditional matching efficiency used in single-port antennas. In multiport antennas, the matching efficiency

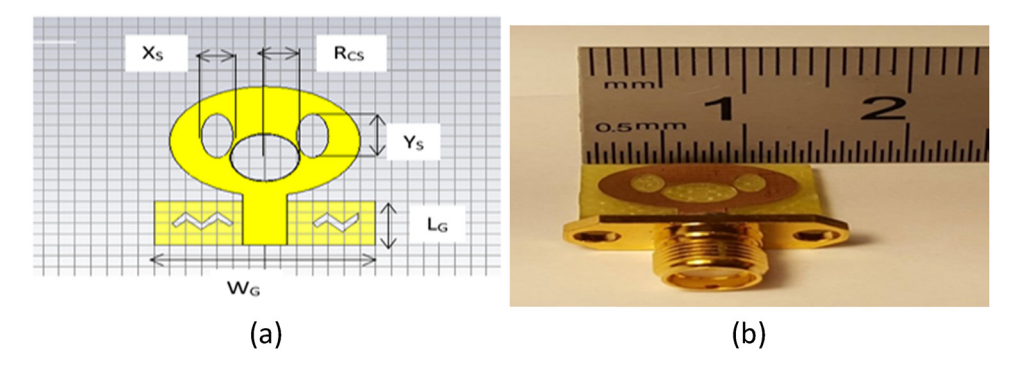


Figure 4: Single-port antenna: (a) simulated and (b) manufactured.

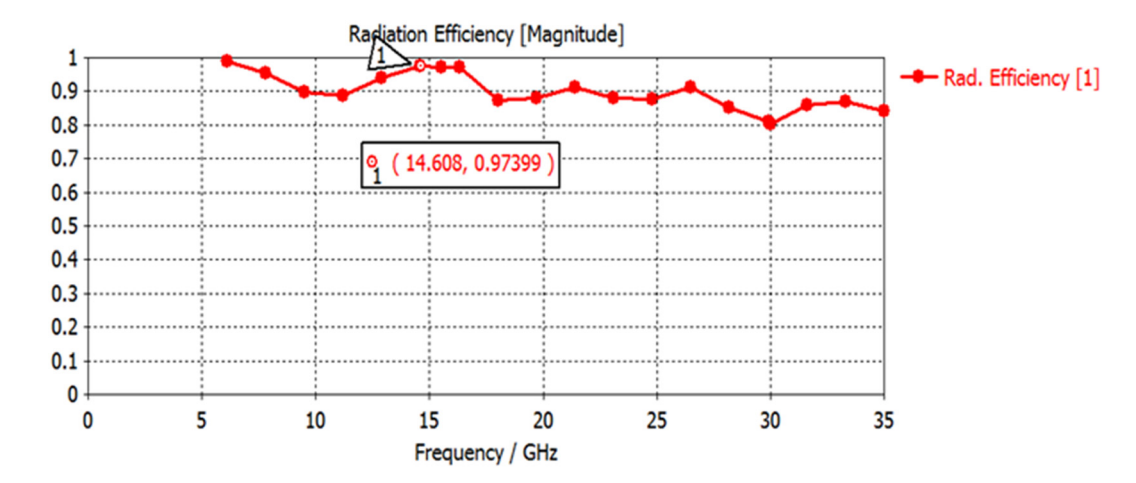


Figure 5: Maximum radiation efficiency for a single-port antenna.

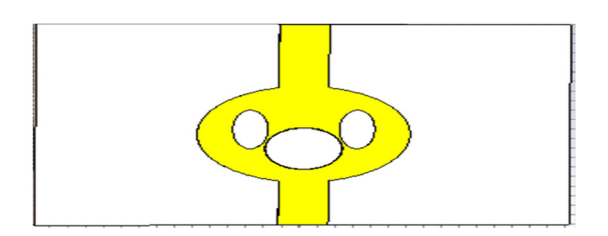


Figure 6: Two-port antenna configuration.

represents the corresponding ratio of the power acceptance to the maximum power available. In this study, we denote this useful efficiency metric by  $e_{\rm mp}^i$ . The three-efficiency metrics are proportional as follows:

$$e_{\rm mp}^i e_{\rm tot}^i = e_{\rm mp}^i \cdot e_{\rm emb}^i, \tag{7}$$

where  $e_{\mathrm{mp}}^{i}$  is the ratio of the amount of power radiated to an amount of power accepted, and it is defined as the

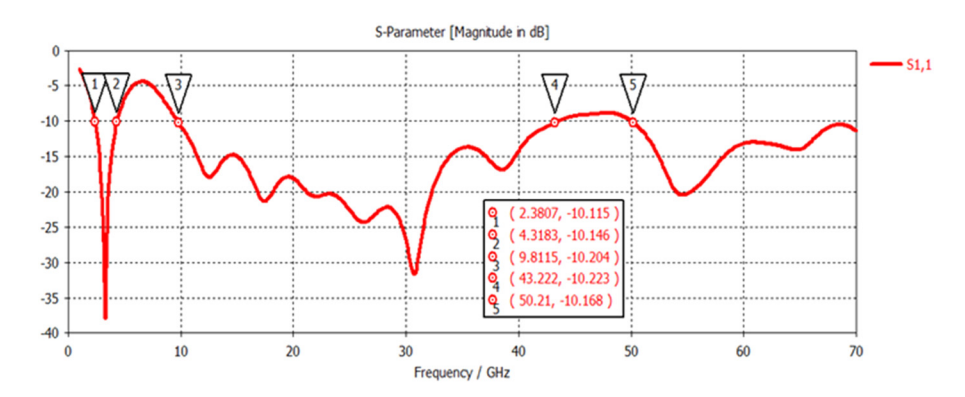


Figure 7: Port 1 reflection coefficient S11.

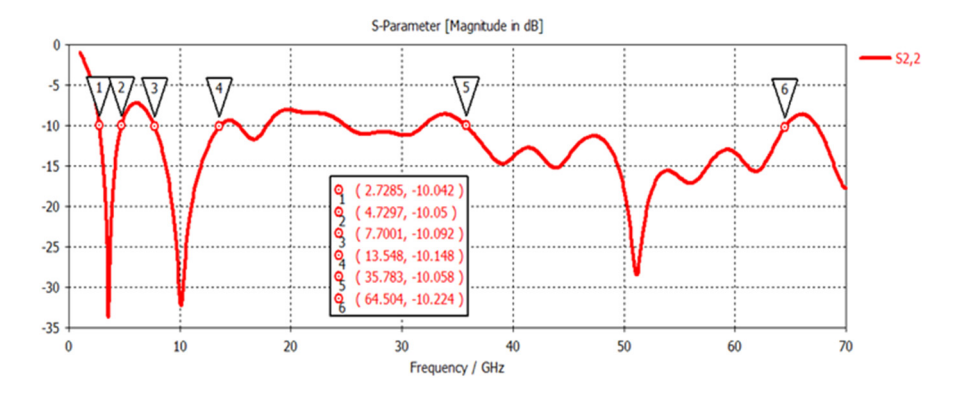


Figure 8: Port 2 reflection coefficient S22.

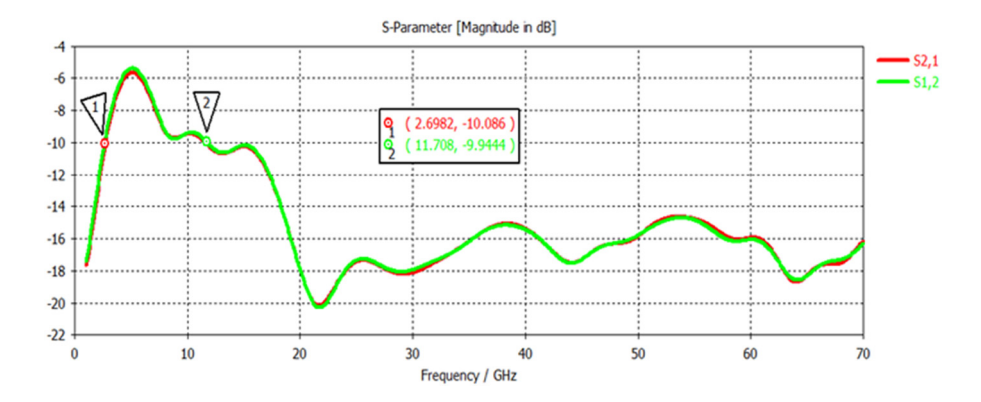


Figure 9: Mutual reflection coefficients S12 and S21 for the two ports.

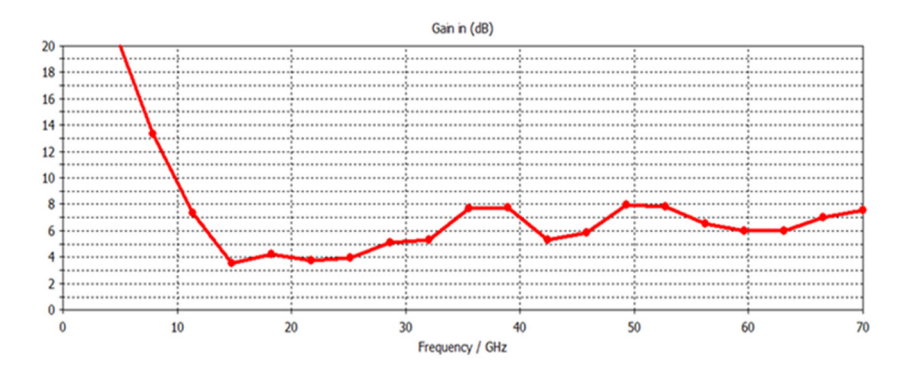


Figure 10: Maximum gain of the antenna.

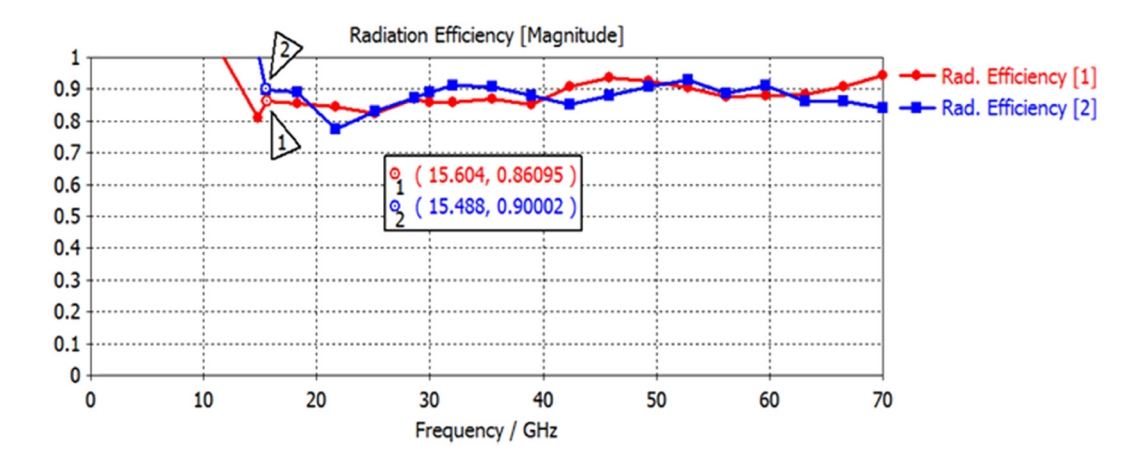


Figure 11: Radiation efficiencies of the antenna.

embedded efficiency for port i when the port i is excited and the other ports are ending [14].

### 3.3 Two-port antenna

Nowadays, the antenna design for mobile phones is a very precise process. Many communication applications

are integrated into the same device and can offer multiple services such as GPS, WLAN services, etc., all of which rely on a multi-band antenna. Since mobile phones are small in size, designing an antenna that meets the requirements of these smart phones is a challenging issue due to the limited space and cost [16–22].

In this part, an antenna with two input ports is presented. Each port produces different frequency bands. The

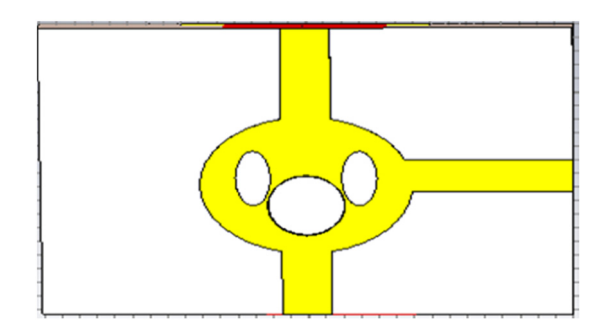


Figure 12: Three-port antenna configurations.

proposed antenna is implemented in an area of 315 mm<sup>2</sup>. FR-4 is used as a substrate element. A sufficient isolation is required between the ports to operate at the same time. To reduce signal interference, the polarization of each port was set to 180° out of phase from one another for the proposed antenna. This solution is suitable for the configuration of the system required for multiple services, and it increases the capacity to transfer and process data.

Due to the small size of the antenna, it can be effectively integrated inside the phone using the standard printed circuit board. The antenna is fabricated using

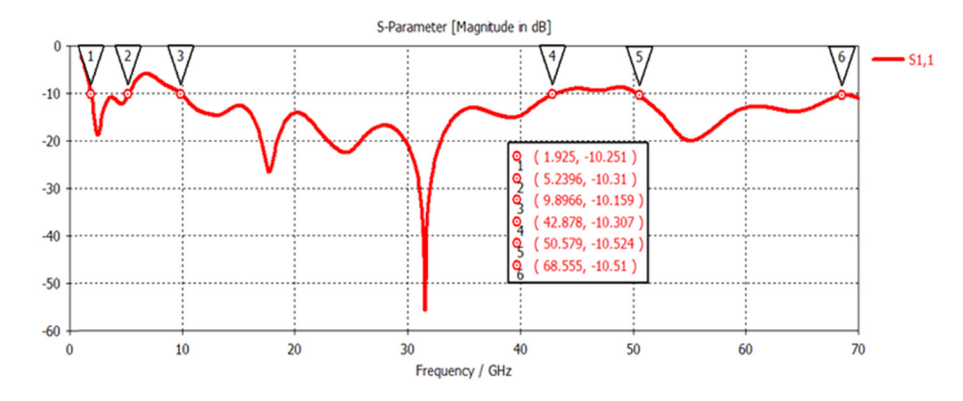


Figure 13: Reflection coefficient for port 1 (S11) of the three ports antenna.

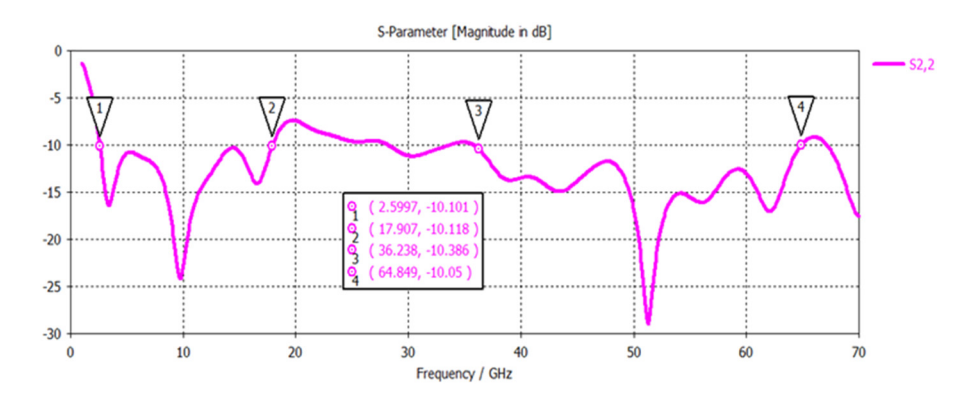


Figure 14: Reflection coefficient for port 2 (S22) of the three ports antenna.

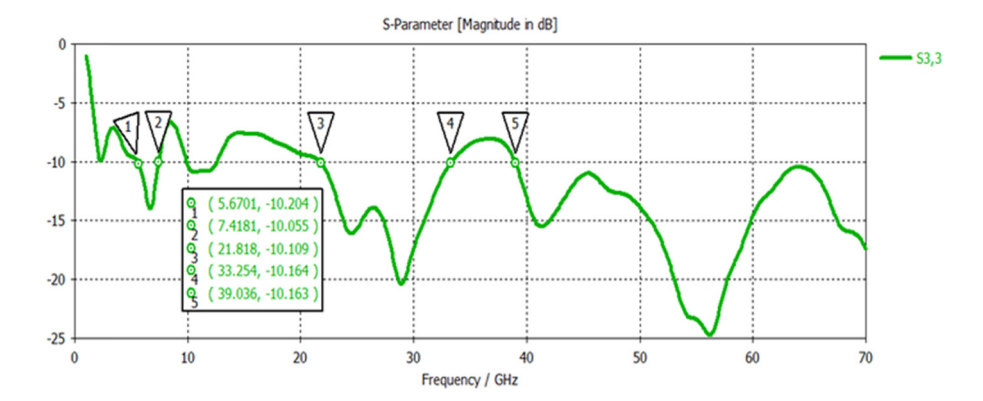


Figure 15: Reflection coefficient for port 3 (S33) of the three ports antenna.

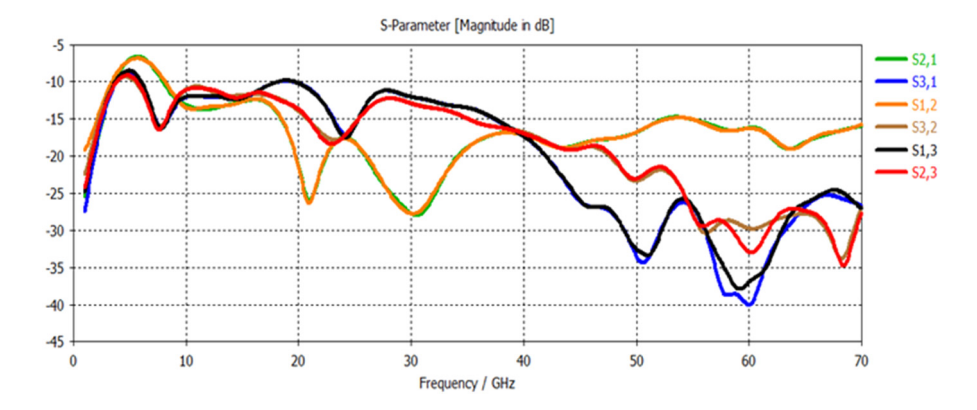
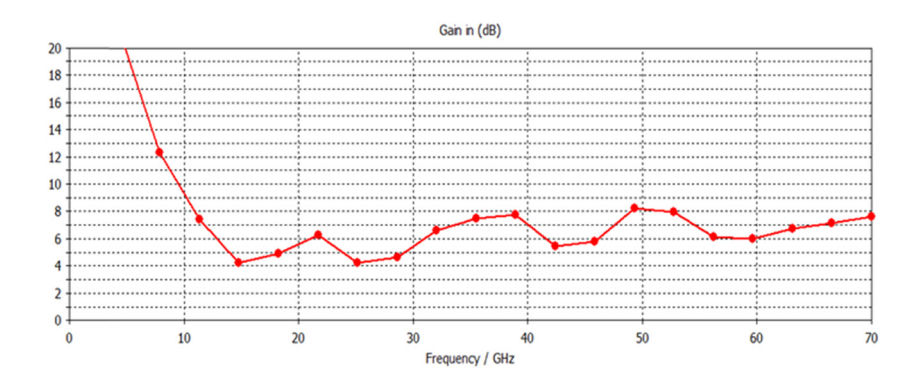


Figure 16: Mutual reflection coefficients for the three-port antenna.



 $\textbf{Figure 17:} \ \ \textbf{Gain variation with frequency for the three-port antenna.}$ 

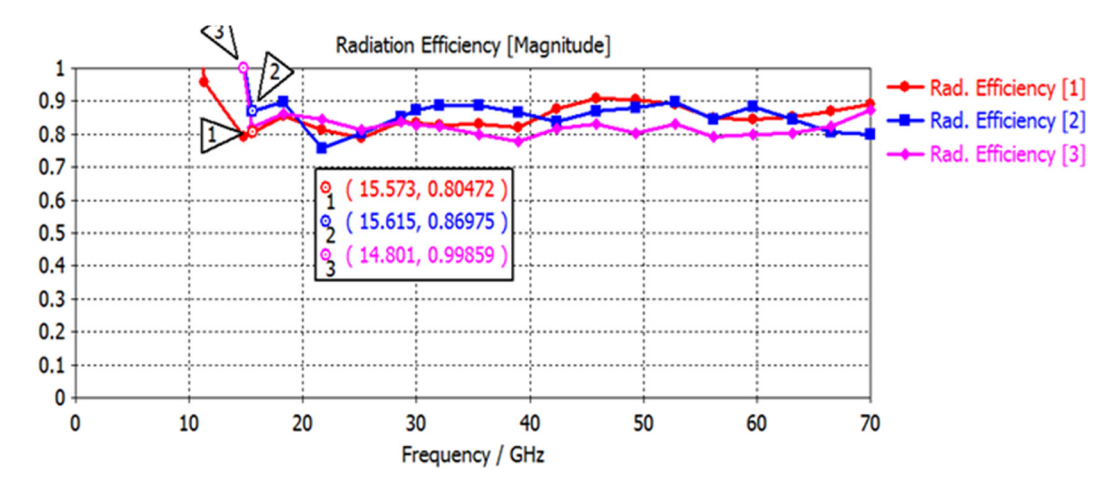


Figure 18: Radiation efficiency of the three-port antenna.

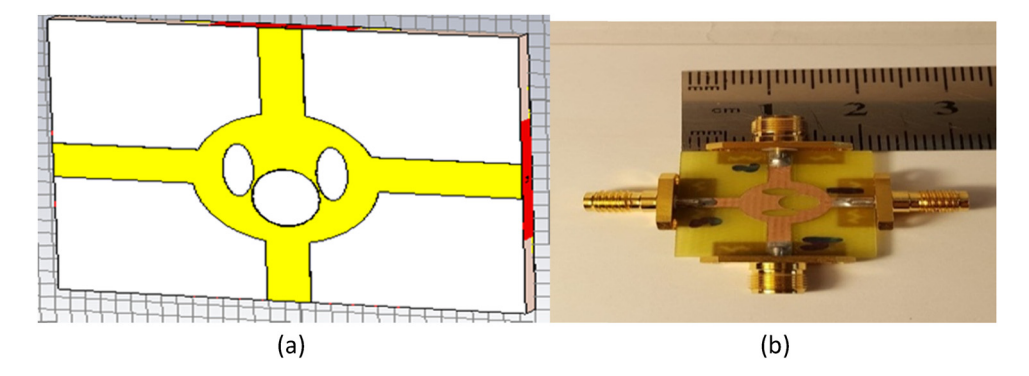


Figure 19: The proposed antenna: (a) simulated and (b) fabricated.

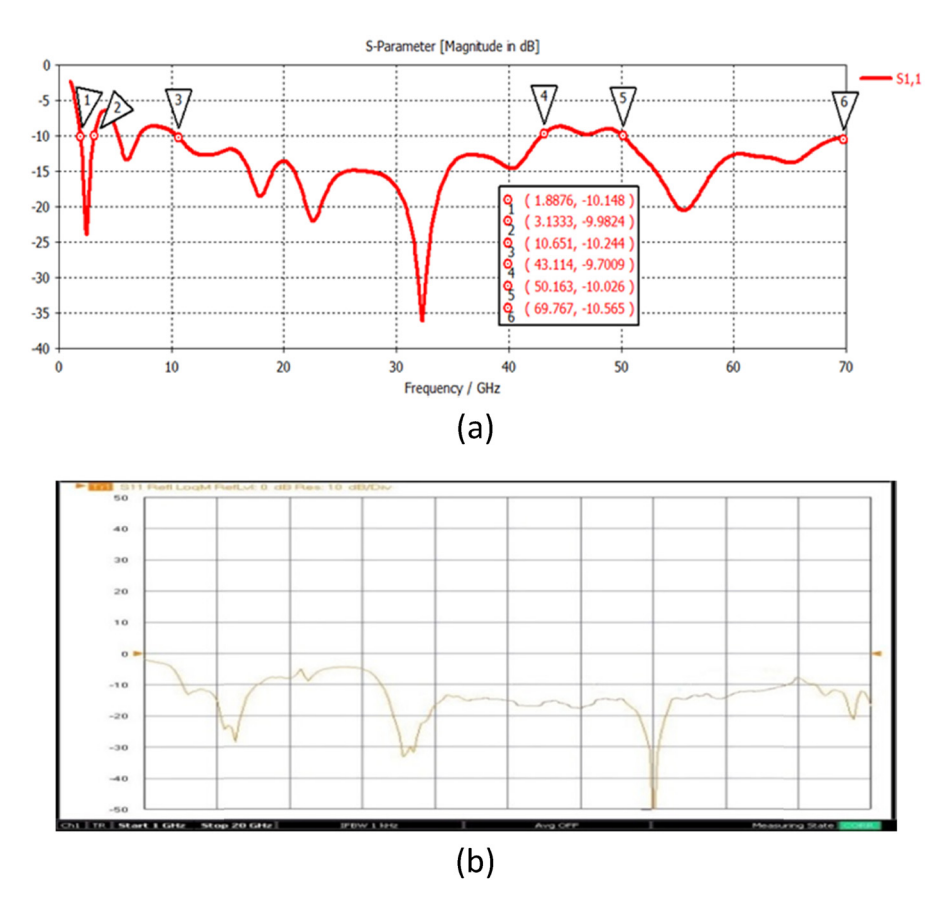


Figure 20: S11 for four-port antenna: (a) simulated and (b) measured.

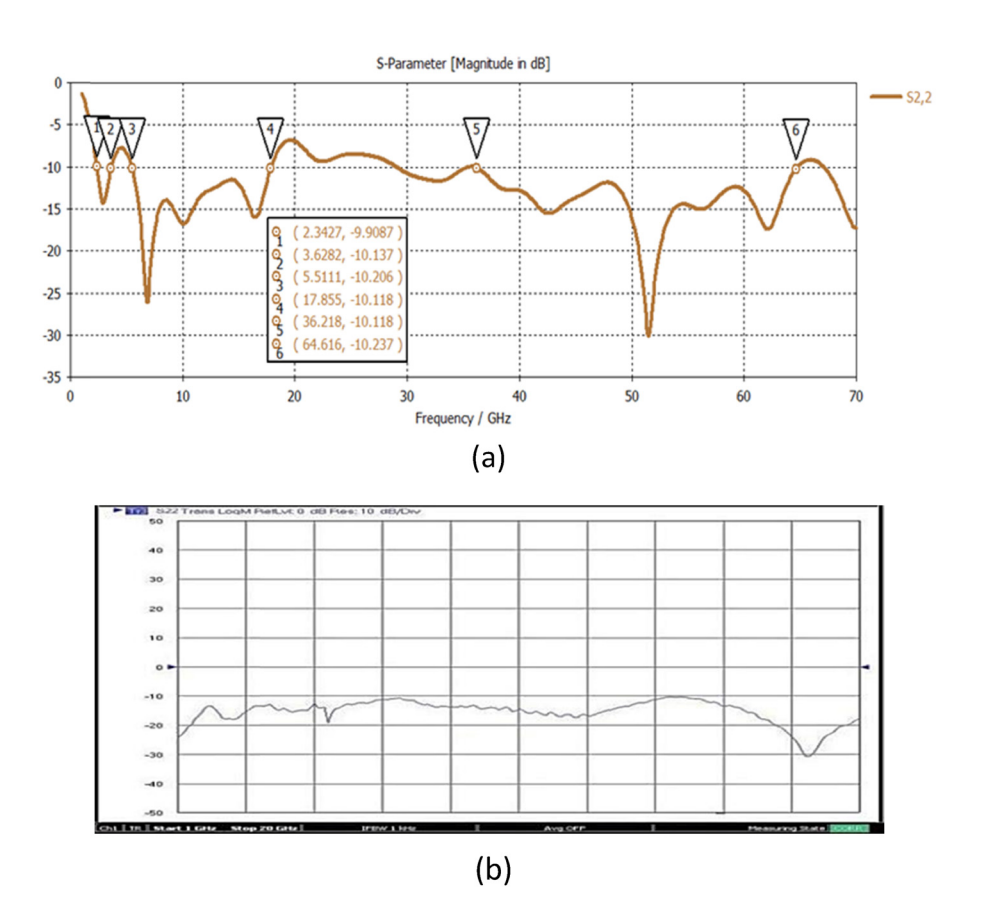


Figure 21: S22 for four ports antenna: (a) simulated and (b) measured.

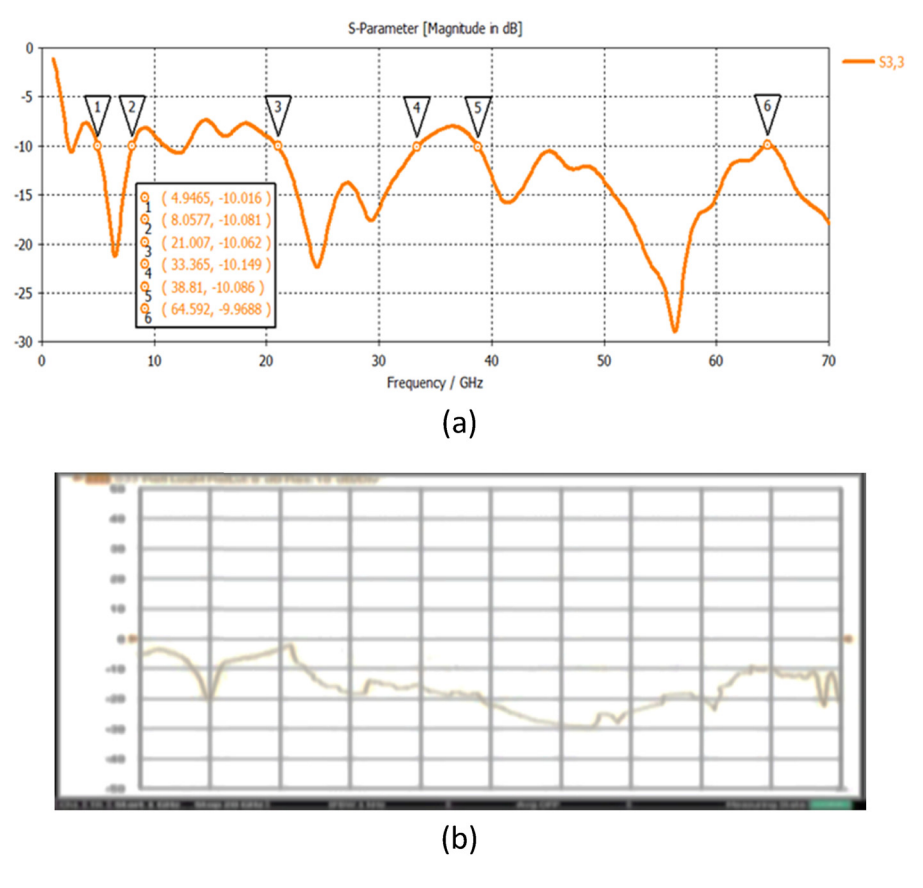


Figure 22: S33 for four ports antenna: (a) simulated and (b) measured.

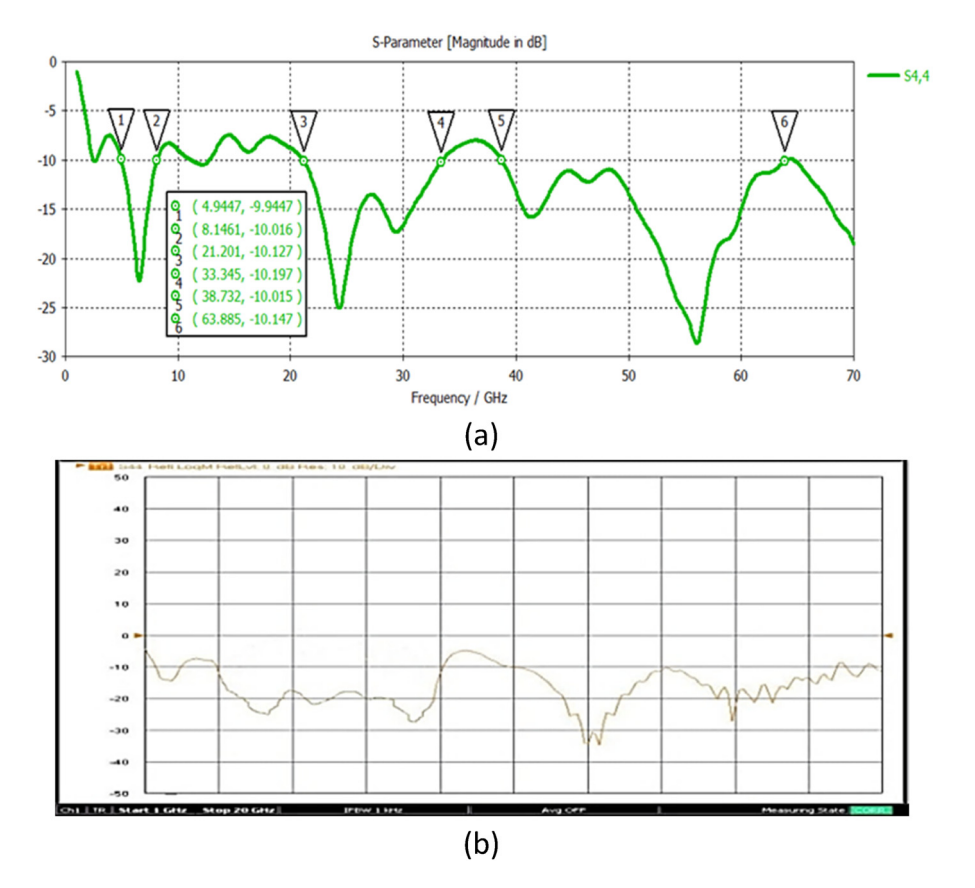


Figure 23: S44 for four ports antenna: (a) simulated and (b) measured.

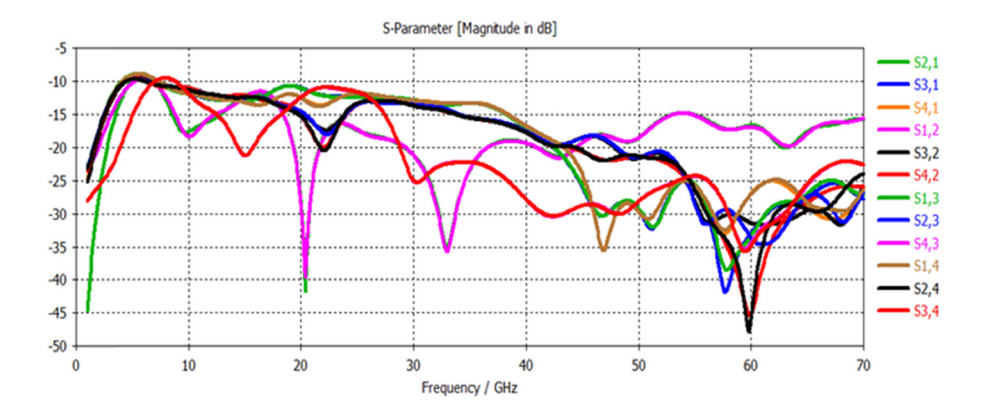


Figure 24: Mutual reflection coefficients S21, S31, S41, S12, S32, S42, S13, S23, S43, S14, S24, and S34 of four-port antenna.

**Table 1:** The minimum value of mutual reflection coefficient for four ports

Minimum mutual reflection coeffici	ent Value (dB)
S12	40
S13	38
S14	36
S21	42
S23	40
S24	47
S31	43
S32	42
S34	47
S41	35
S42	47
S43	41

FR-4 substrate with a relative permittivity  $\varepsilon_r = 4.3$ , dissipation factor tan  $\delta = 0.002$ , and thickness of 1.6 mm. The ground layer is implemented, as copper layer with 0.035 mm, in an area of 315 mm<sup>2</sup>. A new modification has been proposed by linking two physically separate ports (180° angle) as presented in Figure 6. Each port resonates at different frequency bands within a wideband suitable for the 5G

broadband applications. Port 1 multiband simulation results are 2.3–4.3, 9.8–43.2, and 50.2–70 GHz. Port 2 multiband simulation results are 2.7–4.7, 7.7–13.5, and 35.7–64.5 GHz.

The proposed two port antenna is simulated in Computer Simulation Technology (CST) software. The reflection coefficients (S11) and (S22) are shown in Figures 7 and 8, respectively. Mutual reflection coefficients (S12), (S21) are presented in Figure 9. Maximum gain is around 8 dBi as presented in Figure 10. The radiation efficiency for port 1 is 86% and port 2 is 90% as depicted in Figure 11.

#### 3.4 Three-port antenna

A new model has been proposed with three physically separate ports as shown in Figure 12. This configuration results in three different frequency bands. Since the antenna area is limited, the ports must be placed orthogonally to reduce the mutual effect of each other. The simulation results of the reflection coefficients S11, S22, and S33 are shown in Figures 13–15 respectively. For S11, the bands are: 1.9–5.2, 9.89–42.8, and 50.5–68.5 GHz. For

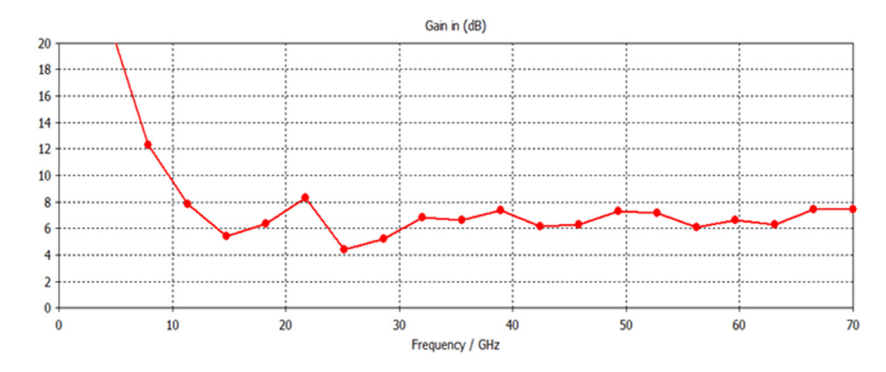


Figure 25: Gain variation with frequency of the four-port antenna.

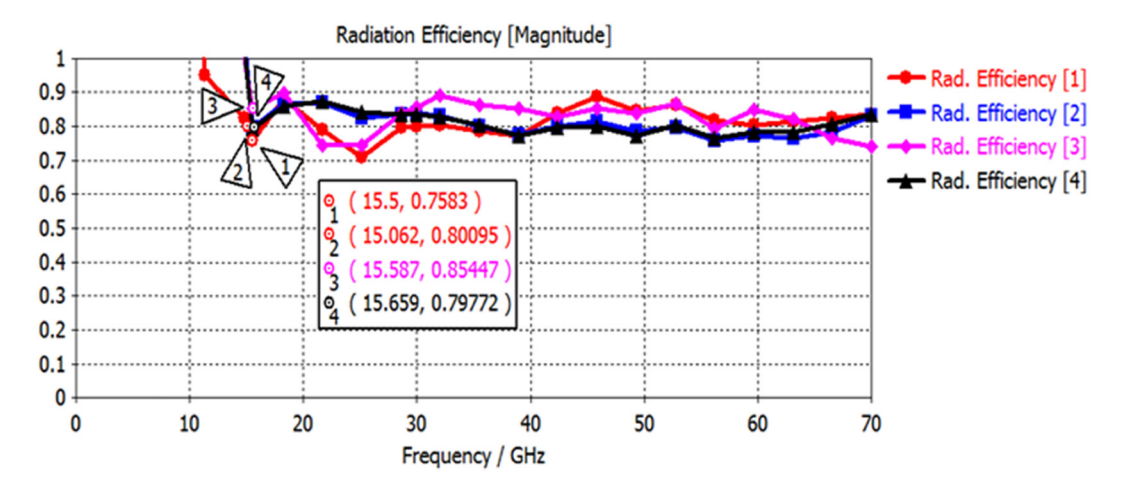


Figure 26: Radiation efficiencies for four-port antenna.

S22, the bands are: 2.5–17.9, and 36.2–64.8 GHz, while for S33, the bands are: 5.6–7.4, 21.8–33.2, and 39–70 GHz.

The mutual reflection coefficients S12, S13, S21, S23, S31, and S32 are shown in Figure 16, while the gain of 8 dBi was obtained as shown in Figure 17. Also, the radiation efficiencies for the three ports are 80, 86, and 99% for ports 1, 2, and 3, respectively, as shown in Figure 18.

#### 3.5 Four-port antenna

A four-port antenna was designed, implemented, and manufactured for wireless communication applications. The design does not require any other separation structure to achieve insulation between multiple ports due to the use of four polarized ports. A combination of four port units produces an elliptical shape. This elliptical patch which contained four-ports was manufactured using the orthogonal technique, the phase difference between Ports 1 and 3 was 180° on the *X*-axis polarization. Likewise, the phase difference between Ports 2 and 4 was also 180° on the *Y*-axis polarization to prevent interference between them. The equations of the waves moving in a certain direction regardless of the orientation of the waves traveling in the opposite direction are

$$E_V = \widetilde{a}_X(E_0 e^{-\gamma y})$$
 For port 1, (8)

$$E_{-\nu} = \tilde{a}_x (E_o e^{-\gamma y})$$
 For port 3, (9)

$$E_x = \overline{a}_y (E_o e^{-yx})$$
 For port 2, (10)

$$E_{-x} = \tilde{a}_{\nu}(E_0 e^{-\gamma x})$$
 For port 4. (11)

The designed and fabricated prototype of the fourport antenna is shown in Figure 19. The simulation and practical result for the reflection coefficients S11, S22, S33, and S44 in are shown in Figures 20(a and b), 21(a and b), 22(a and b), and 23(a and b), respectively. Note that the practical results were obtained by conducting the test of the proposed antenna using 20 GHz vector network analyzer. For S11, the bands are: 1.8–3.1, 10.6–43.1, and 50.1–69.7 GHz. For S22, the bands are: 2.3–3.6, 5.5–17.8, and 36.2–64.6 GHz. For S33, the bands are: 4.9–8, 21–33, and 38–64.6 GHz. And for S44, the bands are: 4.9–8, 21.2–33.3, and 38.7–63.8 GHz.

Mutual reflections coefficient S12, S13, S14, S21, S23, S24, S31, S32, S34, S41, S42, and S43 are shown in Figure 24. Also, Table 1 shows the minimum value of mutual reflection coefficients, which shows the effectiveness of the fourport antenna. The gain is around 8.3 dBi as shown in Figure 25, and the radiation efficiencies are 75, 80, 85, and 79 for ports 1, 2, 3, and 4, respectively, as illustrated in Figure 26.

## 4 Conclusion

The use of a single-port antenna is useful for wireless communication system, such as 5G mobile, where it is used in the transfer and process a large amount of data in mobile networks, since it enables wideband applications and is also lower in size. However, the lower return loss of a single-port antenna reduces the antenna's efficiency. Therefore, in this work, further development of this antenna is made by connecting it to more than one port to increase the number of frequency bands, which reduces the return loss and increases the efficiency.

The CST software was used to simulate two-port, three-port, and four-port antennas which were fabricated

using the orthogonal technique. The phase difference between Ports 1 and 3 was 180° on the *X*-axis polarization, while the phase difference between Ports 2 and 4 was 180° on the *Y*-axis polarization to prevent the interfering between their signals. The experimental results reveal that the created antenna design outperforms the one-port, two-port, and three-port antennas in terms of efficiency. The proposed four-port antenna returns the following losses: The bands for S11 are 1.8–3.1, 10.6–43.1, and 50.1–69.7 GHz, while the bands for S22 are 2.3–3.6, 5.5–17.8, and 36.2–64.6 GHz, and the bands for S33 are: 4.9–8, 21–33, and 38–64.6 GHz. The bands for S44 are 4.9–8, 21.2–33.3, and 38.7–63.8 GHz. The antenna design was improved to enhance the bandwidth and radiation efficiency.

**Conflict of interest:** Authors state no conflict of interest.

## References

- Aronsson D. Channel estimation and prediction for MIMO OFDM systems: Key design and performance aspects of kalman-based algorithms. Uppsala universitet, Sweden: Institutionen for Teknikvetenskaper; 2011.
- [2] Cripps SC. RF power amplifiers for wireless communications. (Artech House Microwave Library (Hardcover)). Norwood, MA, USA: Artech House, Inc; 2006.
- [3] WC J Jr. Microwave mobile communications. New York: Wiley; 1974.
- [4] Goldsmith A. Wireless communications. Cambridge, UK: Cambridge University Press; 2005.
- [5] Vaughan R, Andersen JB. Channels, propagation and antennas for mobile communications. let. 2003;50:50.
- [6] Abbosh AM, Bialkowski ME. Design of ultrawideband planar monopole antennas of circular and elliptical shape. IEEE Trans Antennas Propag. 2008;56:17–23.
- [7] Jassim AK, Thaher RH. Design and analysis of broadband elliptical microstrip patch antenna for wireless communication. TELKOMNIKA (Telecommun Comput Electron Control). 2018;16:27.
- [8] Abdullah AS, Ali RS, Wali MH. Design and analysis of compact H-like element microstrip reflectarray antenna for X-band applications. Br J Appl Sci & Technol. 2014;4(34):4807.

- [9] Wali MH, Jassim AK, Almgotir HM. Design and analysis 5G mobile network model to enhancement high-density subscribers. Bull Electr Eng Inform. 2021;10(3):1464-74.
- [10] Abdullah LW, Wali MH, Saloomi AH. Twelfth mode on-demand band notch UWB antenna for underlay cognitive radio. Indonesian J Electr Eng Comput Sci. 2021;22(3):1446-56.
- [11] Abdullah LW, Sallomi AH, Wali MH. A sixteen mode frequency reconfigurable antenna for underlay cognitive radio. 2021 IEEE 19th Student Conference on Research and Development (SCOReD); 2021. p. 146–51. doi: 10.1109/SCOReD53546.2021.9652735.
- [12] Ivashina MV, Kehn MNM, Kildal P-S, Maaskant R. Decoupling efficiency of a wideband Vivaldi focal plane array feeding a reflector antenna. IEEE Trans Antennas Propag. 2009:57:373-82.
- [13] Stein S. On cross coupling in multiple-beam antennas. IRE Trans Antennas Propag. 1962;10:548-57.
- [14] Luomaniemi R, Ylä-Oijala P, Lehtovuori A, Viikari V. Q-factor for multiport antennas and achievable bandwidth estimation. IEEE Trans Antennas Propag. Oct. 2021;69(10):6364–73. doi: 10.1109/TAP.2021.3070115.
- [15] Raad ZSJ, Thaher H. Design of dual band microstrip antenna for Wi-Fi and WiMax applications. TELKOMNIKA. December 2018 2018;16:2864-70.
- [16] Jassim AK, Thaher RH. Enhancement gain of broadband elliptical microstrip patch array antenna with mutual coupling for wireless communication. Indonesian J Electr Eng Comput Sci. january 2019;13:217–25.
- [17] Saada MHA. "Design of Efficient Millimeter Wave Planar Antennas for 5G Communication Systems." The Islamic University-Gaza; 2017.
- [18] Satrusallya S, Mohanty MN. Design of an array antenna for 5G wireless network with enhanced bandwidth. Infocom Technologies and Unmanned Systems (Trends and Future Directions) (ICTUS), 2017 International Conference on; 2017. p. 1–5.
- [19] Zhu S, Liu H, Chen Z, Wen P. A compact gain-enhanced vivaldi antenna array with suppressed mutual coupling for 5G mmWave application. IEEE Antennas Wirel Propag Lett. 2018;17:776-9.
- [20] Lopez DG, Al-Tarifi MA, Lasser G, Filipovic DS. Wideband antenna systems for millimeter-wave amplitude-only direction finding. Trans Antennas Propag. 2018;66(6):3122–9. doi: 10.1109/TAP2823779.
- [21] Saxena S, Kanaujia B, Dwari S, Kumar S, Tiwari R. MIMO antenna with built-in circular shaped isolator for sub-6 GHz 5G applications. Electron Lett. 2018;54:478–80.
- [22] Majidzadeh M. Linear and circular polarization radiation through a modified 270° square ring-fed  $2\times 2$  array antenna. AEU-Int J Electron Commun. 2019;98:164–73.